TORSIONAL DEFORMATION OF <111> AXIALLY ORIENTED Cu NANOWIRES

A. Luque, J. Aldazabal, J.M. Martínez-Esnaola, J. Gil Sevillano

CEIT and Tecnun (University of Navarra)
Paseo Manuel de Lardizábal 15, 20018 San Sebastián (Spain)
E-mail: aluque@ceit.es Tel.: 34 943 21 28 00 Fax: 34 943 21 30 76

Molecular Dynamics simulations of the torsional deformation of cylindrical <111> axially oriented single crystalline copper nanowires of different diameters have been performed using the *embedded-atom method* [1, 2], where each atom is considered as an "impurity" occupying a site of the lattice formed by the rest of atoms. The atoms experience two types of interactions, as shown in eq. (1): through a *pair potential V*, with the atoms around it, and because of their electrons, through an *embedding potential F* dependent on the relative electronic density ρ, which is calculated with eq. (2).

$$E_i = \frac{1}{2}\sum_{j\neq i} V\left(r_{ij}\right) + F\left(\rho_{ti}\right) \quad (1)$$

$$\rho_{ti} = \sum_{j\neq i} \rho\left(r_{ij}\right) \quad (2)$$

Tabulated data for the embedding and pair potentials for copper are taken from ref. [3]. Forces on each atom are calculated from eq. (1) and their trajectories are computed numerically [4].

For the present work, 5 cylindrical [111] axially oriented copper nanowires (fig. 1) of diameters ranging from 1.5 to 20 nm and lengths ranging from 2.5 to 25 nm were generated. The specimens are periodic along the *z*-axis in order to avoid border effects in this direction. The simulations are carried out at 300 K using time steps of 2.5 fs. The surface shear strain rates used for the simulations ranged from $3\cdot10^8$ s^{-1} for the smallest specimens to $4\cdot10^8$ s^{-1} for the largest. This range is small enough to attribute differences between specimens behaviour to strain rate effects. A constant twist of opposite sense is applied to the ends of the cylinder during the test. After each step, the force on each atom is derived from the potential and atoms are moved towards their new position. A velocity-scaling technique [5] is used for maintaining the system temperature equal to 300 K.

Figure 2 shows the nominal shear stress vs. shear strain obtained from the simulations (calculated from the torque-twist response assuming elastic behaviour). In all cases, we first observe an elastic regime followed by plastic yielding at a shear yield stress τ_y. Figure 3 summarizes the results obtained in these tests. The value of the shear modulus *G* for the larger diameters matches reasonably well with the one found in the literature for {111}<uvw> shear of bulk copper crystals at 300 K [6]. Both *G* and τ_y depend on the specimen size. We are in presence of surprising "reverse" size effect: the smaller is softer and more compliant. The higher fraction of surface atoms in the smaller diameters probably explains their lower shear modulus. Moreover, if we normalize the yield stress τ_y with *G* (fig. 4) we obtain a weak but "normal" size effect, of the same type found in tension, and therefore "the smaller, the stronger" in the plastic regime [7]. This effect comes from the probability of nucleation of dislocations from the free surface, increasing with size in the geometrically similar wires.

Another important feature of these simulations is the storage of geometrically necessary dislocations (GND) to accommodate the torsional deformation, as shown in fig. 5.b in comparison with fig. 5.a. The plastic shear is localised in a very thin zone where the GND density grows until the twist reaches 30º decreasing thereafter (fig. 5.c), until total dislocation starvation takes place for 60º when the upper and lower crystal pieces perfectly match again (fig. 5.d). GNDs form a twist boundary of increasing misorientation. For larger diameters the GND sub-boundary is better observed (fig. 6.a).

References:

[1] Daw M.S., Baskes M.I., "Semiempirical, Quantum Mechanical Calculation of Hydrogen Embrittlement in Metals", Phys. Rev. Lett., 50, 1258-1288 (1983).
[2] Daw M.S., Baskes M.I., "Embedded-atom method: Derivation and application to impurities, surfaces, and other defects in metals", Phys. Rev. B, 29, 6443-6453 (1984).
[3] Mishin Y., Farkas D., Mehl M.J., Papaconstantopoulos D.A., "Structual stability and lattice defects in copper: Ab initio, tight-binding, and embedded-atom calculations", Phys. Rev. B, 63, 224106 (2001).
[4] Raabe D., "Computational Materials Science", Wiley-VCH, 101-102 (1998).

[5] Rapaport D.C., "The Art of Molecular Dynamics Simulation", Cambridge University Press, 65 (2001).
[6] Frost H.J., Ashby M.F., "Deformation-Mechanism Maps: the plasticity and creep of metals and ceramics", Pergamon Press, 21 (1982).
[7] Horstemeyer M.F., Baskes M.I., Plimpton S.J., "Length scale and time scale effects in the plastic flow of FCC metals", Acta Mater., 49, 4363-4374 (2001).
[8] Li J., "AtomEye: an efficient atomistic configuration viewer", Modelling Simul. Mater. Sci. Eng., 11, 173-177 (2003).

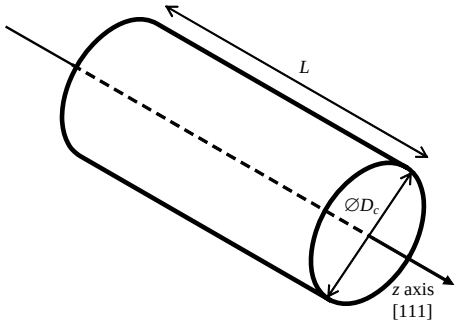

Fig. 1. Geometric characteristics of the tested specimen.

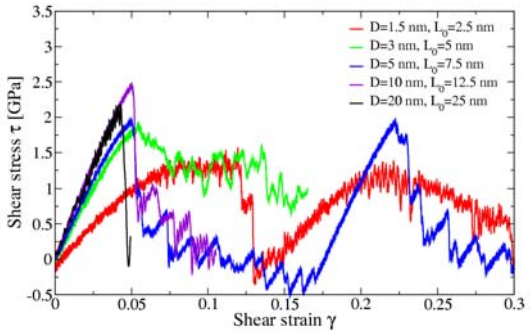

Fig. 2. Nominal shear stress – shear strain plot obtained for the simulated samples.

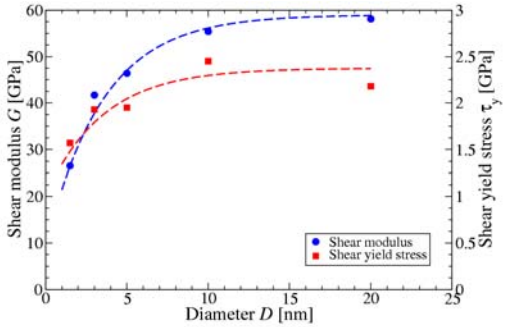

Fig. 3. Dependence of G (scale on the left) and τ_y (on the right) with the specimen size, showing a "reverse" size effect.

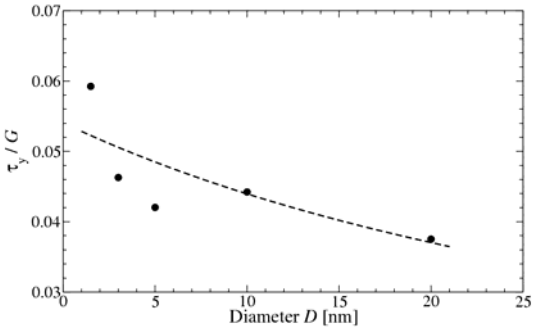

Fig. 4. Dependence of the τ_y/G ratio with the specimen size, showing a "direct" size effect.

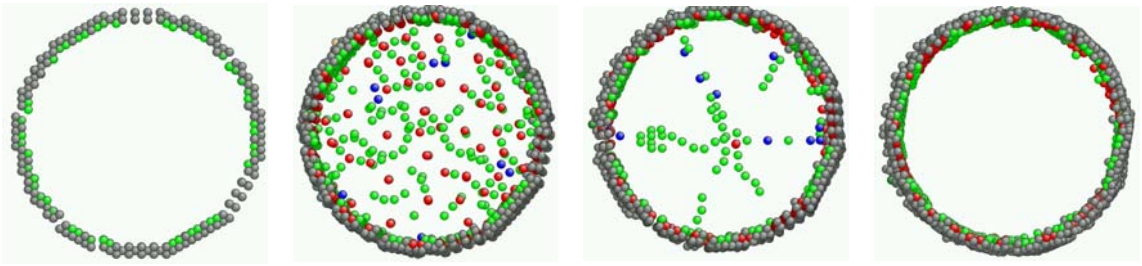

Fig. 5. Cross sections of the D_c=5 nm nanowire for (a) γ=0, (b) γ=0.075, (c) γ=0.15 and (d) γ=0.20. Atoms with coordination number equal to 12 are eliminated for visualization purposes. In red, green and blue, atoms with coordination number equal to 10, 11 and 13. In grey, other coordination numbers [8].

Fig. 6. a) Cross section of the D_c=20 nm nanowire for γ=0.04 showing the GND dislocations that form a disordered twist sub-boundary. See Figure 5 for the colour code. b) Side view.